reactions

MDPI

Article

Heterogeneously Catalyzed γ-Valerolactone Hydrogenation into 1,4-Pentanediol in Milder Reaction Conditions

Irina Simakova [1,2,*], Yulia Demidova [1,2], Mikhail Simonov [1,2], Sergey Prikhod'ko [1,2], Prashant Niphadkar [3], Vijay Bokade [3], Paresh Dhepe [3] and Dmitry Yu. Murzin [4,*]

1 Boreskov Institute of Catalysis, pr. Lavrentieva, 5, 630090 Novosibirsk, Russia; demidova@catalysis.ru (Y.D.); smike@catalysis.ru (M.S.); spri@catalysis.ru (S.P.)
2 Novosibirsk State University, Pirogova 2, 630090 Novosibirsk, Russia
3 CSIR-National Chemical Laboratory, Dr. Homi Bhabha Road, Pune 411008, India; ps.niphadkar@ncl.res.in (P.N.); vv.bokade@ncl.res.in (V.B.); pl.dhepe@ncl.res.in (P.D.)
4 Johan Gadolin Process Chemistry Centre, Åbo Akademi University, Biskopsgatan 8, FI-20500 Turku/Åbo, Finland
* Correspondence: simakova@catalysis.ru (I.S.); dmurzin@abo.fi (D.Y.M.)

Received: 20 September 2020; Accepted: 14 October 2020; Published: 16 October 2020

Abstract: Hydrogenation of γ-valerolactone (GVL) in polar solvents (*n*-butanol, 1,4-dioxane) to 1,4-pentanediol (PDO) and 2-methyltetrahydrofuran (MTHF) was performed at 363–443 K in a fixed bed reactor under overall H_2 pressure of 0.7–1.3 MPa. Preliminary screening in a batch reactior was performed with a series of Ru, Ir, Pt, Co, and Cu catalysts, earlier efficiently applied for levulinic acid hydrogenation to GVL. The fresh catalysts were analyzed by transmission electron microscopy (TEM), X-ray fluorescent analysis (XRF), temperature programmed reduction by H_2 (H_2-TPR), and N_2 physisorption. Cu/SiO_2 prepared by reduction of copper hydroxosilicate with chrysocolla mineral structure provided better selectivity of 67% towards PDO at 32% GVL conversion in a continuous flow reactor. This catalyst was applied to study the effect of temperature, hydrogen pressure, and contact time. The main reaction products were PDO, MTHF, and traces of pentanol, while no valeric acid was observed. Activity and selectivity to PDO over Cu/SiO_2 did not change over 9 h, indicating a fair resistance of copper to leaching.

Keywords: 1,4-pentanediol; γ-valerolactone; hydrogenation; biodiols; Cu; Co; Ir; Re; Pt; Ru; biomass conversion

1. Introduction

Nowadays, lignocellulose-derived carboxylic acids are widely involved as starting materials for the production of commercial chemicals and transport fuel additives [1–3]. Levulinic acid (LA) is considered to be the platform molecule that can be converted into different value-added chemicals [4]. Volatility of fossil fuels prices and their current relatively low levels [5] make alternative, i.e., biomass-derived, fuels not competitive pricewise with counterparts on the basis of petroleum; therefore, production of high value-added chemicals from biomass is deemed to be a more efficient strategy than production of biofuels [6]. Among such high value-added chemicals, bio-based polymers could be mentioned as being a feasible alternative to various synthetic polymers currently produced using predominantly crude oil as a feedstock [7]. Moreover, some of the bio-based polymers such as polylactic acid are biodegradable, which is another advantage of their utilization. On the contrary, production of petroleum-based polymers is largely unsustainable, calling for their efficient recycling. Otherwise, a large increase of waste plastics and, subsequently, environmental pollution are becoming

of tremendous concern [8]. New strategies to replace conventional petroleum-based polymers with renewable alternatives are being developed, involving starting material platform molecules with an appropriate molecular structure derived from biomass, such as agricultural wastes (wheat straw, corn stover) or forest residues. Such biogenic diols, such as 1,4-pentanediol (PDO), can be prepared either from γ-valerolactone (GVL) originating from LA or its esters through hydrogenation or directly from LA esters (Scheme 1). PDO is considered as an alternative bio-derived monomer to produce biodegradable polyesters with a high strength [9], which are globally increasingly in demand [10]. It is worth noting that PDO has wide application areas that are also used as an intermediate in the production of fine chemicals, cosmetics, or pharmaceuticals [11,12].

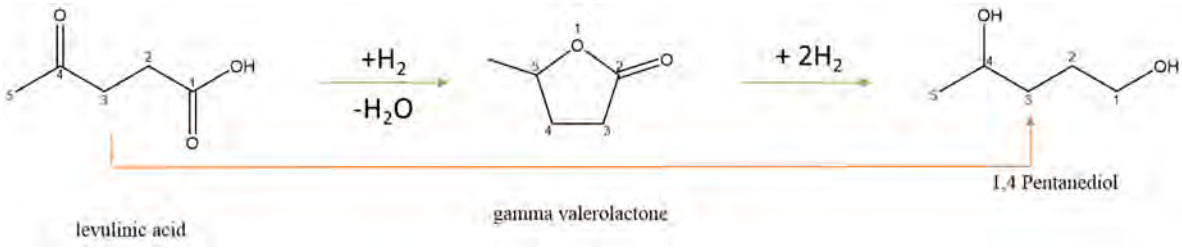

Scheme 1. Possible routes of 1,4-pentanediol (PDO) formation from levulinic acid (LA) and γ-valerolactone (GVL).

Catalytic hydrogenation of GVL to PDO was conducted selectively over homogeneous catalysts on the basis of Ru [10,13,14], Co [15,16], and Fe [17], for which almost 100% product yield was reported. However, from the viewpoint of industrial implementation, homogeneous catalysts are inferior to heterogeneous ones owing to difficulties in separating the catalyst from the reaction media. Some catalysts based on noble metals (Ru [9,18], Pt [19], Rh-MoOx/SiO_2 [20]) were studied in the liquid-phase GVL hydrogenation, not demonstrating a high selectivity for the PDO formation. Hydrogenation of GVL over solid catalysts in a fixed-bed reactor under hydrogen pressure (0.2–2.0 MPa) was reported to proceed over various catalysts based on noble and non-noble metals [21]. The former ones bearing Pd and Pt, as well as nickel-based catalysts, did not result in the desired PDO yield under mild reaction conditions. The highest yield of PDO was achieved over 40 wt.% Cu/ZnO catalyst at 140 °C and pressure of 1.5 MPa, resulting in GVL conversion of 82.3% and selectivity to PDO 99.2%, while at higher temperatures, 2-methyltetrahydrofuran and 1-pentanol were formed. Activity of Cu/ZnO was strongly influenced by the calcination temperature, resulting in a higher activity upon calcination temperature elevation. The use of Cu/MgO catalysts with different copper content was also found to be effective [22]. The optimal physical chemical parameters of the catalyst and reaction conditions were copper loading of 18%, reaction temperature of 473 K, and hydrogen pressure of 10 MPa. Under optimal conditions, the PDO yield was 94.4% at 90.5% GVL conversion. The catalyst displayed stable behavior over 10 h and could be reused. Copper-based catalysts have also been studied in [9,18,23]. Cu/ZrO_2 catalyst demonstrated, for example, a high selectivity of 99% and GVL conversion of 97% at 473 K and hydrogen pressure of 6 MPa [9]. The main drawback of GVL conversion into PDO over copper catalysts supported on ZnO, MgO, and ZrO_2 was a requirement of high hydrogen pressures (6–10 MPa) and elevated temperatures. A number of bifunctional Cu-containing catalysts with the overall composition $Cu_x/Mg_{3-x}AlO$ (x = 0.5, 1, 1.5, 2) were suggested for hydrogenation of various lactones [24]. The highest selectivity was observed for the catalyst with the composition $Cu_{1.5}/Mg_{1.5}AlO$ (i.e., x = 1.5), which was effective in the hydrogenation of lactones with different carbons in the heterocycle. The authors note that this catalyst is featured not only by its high efficiency, but also by a low cost and environmental friendliness. However, low productivity in a batch reactor along with high H_2 pressure was rather unattractive in this case.

In view of the development of a new biorefinery strategy of the one-pot LA hydrogenation into diols, it would be reasonable to select the catalysts, well-known as efficient in levulinic acid (LA) hydrogenation to GVL, for studying GVL conversion into PDO. Recently, catalyst screening in LA

hydrogenation into GVL over Ru/zeolites and Ru/C [25] with 1,4-dioxane (438 K, H_2 pressure ca. 1.6 MPa) displayed high LA conversion and GVL selectivity of such materials in comparison with carbon-based counterparts. Among Ru/zeolites, Ru/H-Beta demonstrated higher LA conversion and an obvious advantage of H-Beta owing to a proper microstructure and acidity [26].

So far, silica supported copper catalytic systems were not studied systematically in GVL conversion, being used, among other catalysts, for comparison with Cu/ZnO in GVL hydrogenation [21], while silica supported catalysts are generally of great interest in a wide range of catalytic reactions. In particular, for the Fischer–Tropsch synthesis [27,28], modified Co/SiO_2 were used, while non-promoted Cu/SiO_2 catalysts were shown to be active in lactic acid and lactate hydrogenolysis into 1,2-propanediol [29], and Cu/SiO_2 promoted catalysts exhibited high activity for oxidation, esters hydrogenolysis, and methanol conversion [30–32].

Herein, a series of supported heterogeneous catalysts were prepared, all of which were known as active and selective in the levulinic acid hydrogenation to GVL, based on both noble metals (i.e., Ir, Pt, and Ru) and non-noble metals (Cu/ZrO_2, Cu/SiO_2, Co/ZnO_2, Co/ZrO_2), and screened in GVL hydrogenation to study their ability to convert GVL into PDO.

The acidic/basic properties of the support are generally considered crucial for achieving high hydrogenation efficiency or tuning the selectivity of the target products for hydrogenation of levulinic acid to PDO [33]. Therefore, in the current work, for catalysts based on noble metals, acidity was introduced by adding a corresponding promoter such as Re ($IrRe/SiO_2$, $IrRe/Al_2O_3$, $IrRe/ZrO_2$, $PtRe/SiO_2$) or by supporting the metal on an acidic support (Ru/H-Beta with the silica to alumina ratio of 30). On the contrary, copper per se is known to be a Lewis acid, not requiring introduction of additional acidity [34].

The influence of reaction variables such as temperature, hydrogen pressure, as well as catalyst stability was studied to show the feasibility of biogenic diols' synthesis from GVL under rather mild reaction conditions similar to levulinic acid/levulinate hydrogenation into GVL.

2. Materials and Methods

2.1. Materials

In this work, reagent grade materials were used, namely, γ-valerolactone (98 wt.%, Sigma Aldrich, St. Louis, MO, USA), silica Aerosil 300, copper nitrate trihydrate (>99 wt.%, Saksk, Russia), cobalt chloride hexahydrate (>99 wt.%, Reactiv, Russia), $IrCl_3$ hydrate (TU 2625-067-00196533-2002 "V.N. Gulidov Krasnoyarsk factory of nonferrous metals, Krasnoyarsk, Russia), rhenium acid $HReO_4$ (TU 38-301-41-137-90 Reachim, Russia), platinum hydrochloric acid hexahydrate H_2PtCl_6 (TU 2612-034-00205067-2003 AURAT, Russia), zirconia (Acros Organics, Fair Lawn, NJ, USA, S_{BET} = 106 m^2/g), γ-alumina (S_{BET} = 146 m^2/g), silica (S_{BET} = 378 m^2/g), urea (>99 wt.%, Cherkassk, Ukraine), nitrogen (≥99.95%), hydrogen (≥99.95%), and argon (≥99.95%). To prepare substrate solution, all solvents, such as 1,4-dioxane (TU 6-09-659-73) and *n*-butanol, were purified by vacuum distillation.

For H-Beta zeolite, sodium aluminate (43.8 wt.% Al_2O_3, 39.0 wt.% Na_2O), as well as silica sol (40 wt.% SiO_2), tetraethylammoniumhydroxide (TEAOH, aq. 30 wt.% solution), sodium hydroxide (AR), and deionized water, were used.

Substrate solutions were prepared and degassed with N_2 before experiments.

2.2. Catalyst Preparation

To obtain H-Beta zeolite, sodium hydroxide and sodium aluminate dissolved in distilled water were loaded into tetraethyl ammonium hydroxide aqueous solution under vigorous stirring, followed by silica sol gradual addition. A homogeneous gel mixture was obtained after stirring the suspension for 5–6 h. The resulting gel with molar composition of 6.0 $(TEA)_2O$:2.4 Na_2O:30.0 SiO_2:Al_2O_3:840.0 H_2O was then placed into a stainless-steel autoclave and subjected to hydrothermal crystallization at 413 K for 98 h. Complete crystallization was followed by cooling to 323–333 K, separating the solid

product, washing with distilled water and ethanol, drying overnight at 383 K, and calcining in air for 10 h at 823 K.

For preparation of other catalysts, namely, 4%Ru/H-Beta, 4%Ir4%Re/SiO_2, 4%Ir4%Re/Al_2O_3, 4%Pt4%Re/SiO_2, 4%Ir/SiO_2, 4%Ir4%Re/ZrO_2, 30%Cu/ZrO_2, 20%Co/ZrO_2, and 20%Co/ZnO, incipient wetness impregnation was applied using corresponding aqueous solutions of the metal precursors (0.1 M). Thereafter, the catalysts were dried at 383 K for 17 h, reduced by molecular H_2 from 298 up to 673 K (623 K for the zeolite supported Ru) with a ramp rate of 2 K/min. To remove the excess of chloride, the catalysts were treated with H_2 over 3 h at 673 K (623 K for Ru/H-beta).

A homogenous deposition–precipitation method was used for preparation of copper on silica. An aqueous slurry consisting of Aerosil 300 silica, copper nitrate trihydrate, and urea was heated from 298 K till 363 K and held at 363 K for 20 h. After cooling, the sediment was separated, washed, dried at 393 K, calcined in air at 723 K, and reduced by molecular hydrogen from 298 K up to 653 K with a ramp rate of 2 K/min. More details on Cu/SiO_2 catalyst preparation and analysis by differential thermal analysis (DTA), differential thermogravimetric analysis (DTG), and X-ray diffraction analysis (XRD) were reported earlier [29].

2.3. Catalytic Experiments

The catalytic experiments on liquid phase hydrogenation of GVL solution in 1,4-dioxane or *n*-butanol (0.44 M) were performed in a stainless-steel autoclave (150 mL) at 393 K and 3.0 MPa with the catalyst loading of 0.10–0.24 g. Elucidation of the mass transfer limitations done in a similar way as for an even faster hydrogenation of LA to GVL confirmed their absence [26].

Fixed bed GVL hydrogenation (10.1 wt.% in *n*-butanol or 1,4-dioxane) was carried out in a downflow reactor under hydrogen flow (80, 167, or 240 cm^3 min^{-1} (NTP, 293 K, 0.1 MPa)) at 363–443 K under hydrogen pressure of 0.7–1.3 MPa. The hydrogenation set-up consisted of a high-pressure pump, a reactor with the thermocouple located in the middle of the catalyst bed, and a cooler. The substrate solution was vaporized in the preheated line and mixed with purified hydrogen, thereafter passing through the catalyst bed. The volatile products were condensed in a trap circumfluous with cold water. Before experiments, catalyst grains (0.5 g, 0.5–0.63 mm) diluted with the inert quartz beads (0.8 g, 0.63–1.6 mm) were loaded to the reactor to avoid overheating because of a high exothermic effect of hydrogenation. Copper hydroxysilicate precursor was preliminary activated in the reductive atmosphere at 653 K for 2 h in a separate reactor, passivated in N_2, and reactivated at 523 K prior to GVL hydrogenation [29].

The weight hourly space velocity (*WHSV*, h^{-1}) was calculated as follows:

$$WHSV = \frac{v_r}{m_{cat}} = \frac{v_s \cdot \rho \cdot \omega}{m_{cat}} \quad (1)$$

where v_r—the substrate flow rate, cm^3/h; v_s—the solution flow rate, cm^3/h; ρ—solution density, g/cm^3; ω—substrate concentration, wt.%; and m_{cat}—mass of catalyst, g.

The contact time (τ, *h*) was defined as follows:

$$\tau = 1/WHSV \quad (2)$$

2.4. Product Analysis

Condensed products were analyzed by gas-liquid chromatographic (GLC) analysis (Chromos GC-1000) using BP20 capillary column (60 m/0.25 mm/0.25 μm, flame ionization detector FID). The temperature was increased from 323 to 483 K with a temperature ramp of 10 K/min. The temperature of the detector and the evaporator was 523 K, and the flow rate of the carrier gas (hydrogen) was 20 cm^3/min. The reaction components were identified by gas chromatography/mass spectrometry using ZB-Wax capillary column (30 m/0.25 mm/0.25 μm) (VG-7070 Gas Chromatography/Mass Spectrometry (GC/MS)) and VF-5ms capillary column (30 m/0.25 mm/0.25 μm) (Agilent 5973N EI/PCI).

The concentration of a compound i after the reaction was defined in the following way:

$$C_i = \frac{S_i \cdot Q_i}{\sum_j S_j \cdot Q_j} \quad (3)$$

where S_i—chromatographic peak area of compound i, mV·s; and Q_i—a response factor.

Conversion of GVL as well as selectivity to the reaction products were defined from the peak areas using GC considering 100% mass balance for carbon containing reaction components. Conversion was estimated as the mole of consumed substrate per mole of the initial substrate. Selectivity to the corresponding product was calculated as the yield of this product to the overall yield of all products.

2.5. Catalysts Characterization

The majority of characterization methods described below, unless specifically mentioned, were performed for the reduced catalysts.

Transmission electron microscopy (TEM) was used to evaluate the size of metal nanoparticles (NPs), while the crystallographic structure and metal content were determined by X-ray diffraction analysis (XRD) and X-ray fluorescent analysis (XRF), respectively. Nitrogen physisorption was applied to determine the microtexture parameters.

TEM images were obtained with a Hitachi-9000 NAR apparatus. The suspension of the catalyst sample in ethanol was placed on a copper grid, followed by ethanol evaporation. At least 150 nanoparticles from the enlarged images were used to calculate the mean particle size and the standard deviation (SD). The average surface diameter (d_s) was calculated according to Equation (4):

$$d_s = \frac{\sum_i n_i d_i^3}{\sum_i n_i d_i^2} \quad (4)$$

The average mass diameter (d_m) was calculated according to Equation (5):

$$d_m = \frac{\sum_i n_i d_i^4}{\sum_i n_i d_i^3} \quad (5)$$

where n_i—a number of particles with diameter d_i.

The content of elements in the samples was measured by XRF (ARL Advant'X spectrometer) with the powder pellet method using undiluted samples (0.5 g) ground and placed in the die (29 mm diameter). To determine the intensities of the lines for elements, the following excitation conditions were applied: a rhodium anode X-ray tube voltage of 50 kV; current of 40 mA; collimator with a divergence of 0.25°; LiF200 crystal was used as a monochromator; scintillation counter was used as a detector; and counting time was 12 s. The concentration of elements in the sample was defined using a semi-quantitative method with a QuantAS program for standard-less analysis.

The microtextural parameters were estimated by nitrogen physisorption at 77 K (Micromeritics Model ASAP 2400). The specific surface area was calculated using the Brunauer-Emmett-Teller (BET) method within the relative partial pressure range of 0.05–0.25.

The diffraction patterns were obtained on a high-resolution powder diffractometer Thermo techno ARL X'TRA (Switzerland) equipped with a copper anode (λ = 1.5418 Å) and a solid-state semiconductor detector, allowing operation without filters and a monochromator. The measurements were carried out by scanning in the range of 2θ values between 10 and 70° with a step of 0.1° and an accumulation time at a point of 10 s. The sizes of the coherently scattering domain (CSD) were determined from broadening of the diffraction peaks. The instrumental broadening of the diffraction lines was taken into account. Such broadening was recorded from the diffraction pattern using the international

standard—α-Al_2O_3 (SRM 1976). The phase analysis was performed using the The International Centre for Diffraction Data (ICDD) PDF-2 database.

2.6. Copper Surface Determination

The area of metallic copper surface in copper catalysts was estimated by titration of the preliminary reduced Cu oxide precursor (H_2, 653 K) using nitrous oxide injected in a pulse-wise mode [35]. Decomposition of the latter over metal copper resulted in dinitrogen formation, which was quantitatively analyzed by GLC on an LKhM-80 chromatograph (NPO Agropribor, Russia) with a heat-conductivity detector using He as a carrier gas. Separation was done with a Porapack Q capillary column (71 m/0.5 mm/0.05 mm). Absence of nitrogen formation was an indication to stop injection of nitrous oxide pulses. The Cu^0 specific surface area was estimated considering the average surface area occupied by one Cu atom is 0.0711 nm^2 and that a release of N_2 molecule corresponds to the oxidation of two Cu atoms. Therefore, the metal surface *S(Cu)* can be calculated as follows:

$$S(Cu) = 14.2 \times 10^{-20}\, \nu\,(N_2) \cdot N_A \quad (6)$$

where $\nu(N_2)$ is the number of nitrogen (mol), and N_A is the Avogadro number.

3. Results and Discussion

3.1. Characterization of Catalysts

GVL hydrogenation was performed out in the presence of catalysts after their preliminary reduction according to the previously developed methods for hydrogenation of various organic substrates [36–40]. In accordance with the obtained TPR data, reduction of the samples at a temperature above 623 K leads to formation of metallic particles for Ru/H-Beta, IrRe/SiO_2, IrRe/Al_2O_3, PtRe/SiO_2, Ir/SiO_2, IrRe/ZrO_2, Cu/ZrO_2, Co/ZrO_2, and Co/ZnO catalysts. The TEM study showed that the samples are characterized by a uniform distribution of particles across the support, and the average surface particle diameter d_s~0.9–2.2 nm representative for all samples (Figure 1, shown for Ru/H-Beta, IrRe/ZrO_2, IrRe/Al_2O_3). It was found by XPS (not shown) that the active components of the catalysts are metal particles with a small fraction of the oxidized metal except Cu/SiO_2, Cu/ZrO_2, Co/ZrO_2, and Co/ZnO, where the fraction of the oxide phase is larger due to easier re-oxidation during exposure to air. These samples were transferred to the reactor under an argon flow, subsequently under reductive reaction conditions, the partially oxidized phase of the active components undergoes complete reduction.

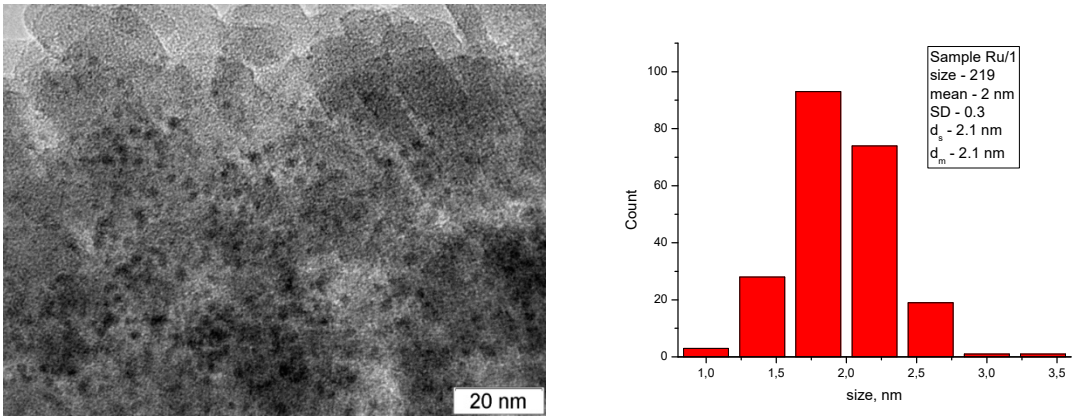

(**a**)

Figure 1. *Cont.*

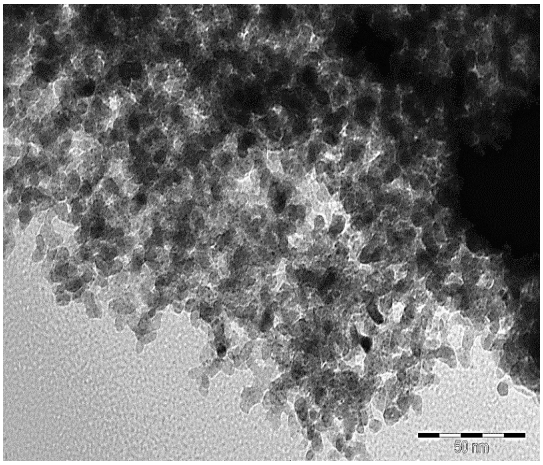

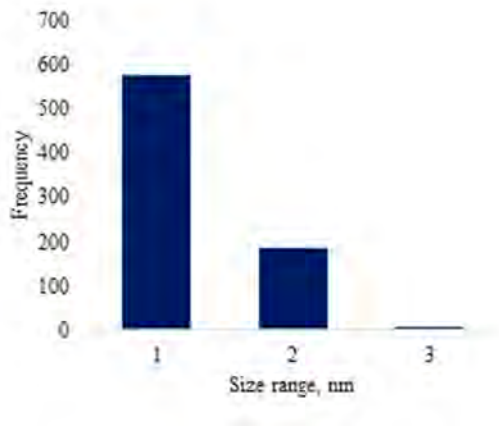

(**b**)

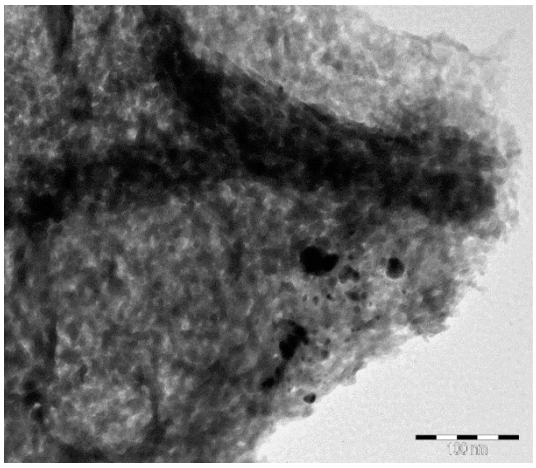

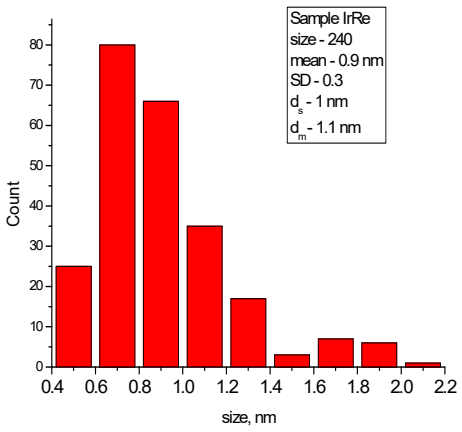

(**c**)

Figure 1. Transmission electron microscopy (TEM) images (**left**) and histograms (**right**) of fresh reduced catalysts: (**a**) Ru/H-Beta; (**b**) 3%IrRe/ZrO_2; and (**c**) 4%Ir4%Re/Al_2O_3.

The catalyst precursor, copper hydroxysilicate with the chrysocolla structure $(CuH)_4[Si_4O_{10}](OH)_8 \cdot nH_2O$, was preliminary activated in a reductive atmosphere at 653 K with a temperature ramp of 2 K/min. The specific surface area of metal copper of carefully reduced Cu/SiO_2 was determined to be 15 m^2/g, while copper loading according to XRF was 45.5 wt.%. The copper on silica catalyst after reduction was characterized by S_{BET} = 520 m^2/g. The crystal phase composition of the reduced Cu/SiO_2 with a minor excess of silica will be discussed in Section 3.3. Earlier, it was shown that reduction of the Cu-Si oxide precursor above 553 K resulted in the formation of highly dispersed Cu^0 particles of 3–8 nm in size, uniformly distributed across the silica surface [41,42].

XRF analysis indicated that the desired metal content with 95% confidence interval was achieved in all catalysts, as expected because of the method of the metal introduction and utilization of the non-volatile precursors.

3.2. Preliminary Catalyst Screening

All prepared catalysts after reductive activation apart from Cu/SiO_2 were preliminary tested in GVL hydrogenation in a batch mode.

The reaction network in GVL hydrogenation generally follows the scheme suggested by Sun et al. [21], where, along with the main reaction products PDO and MTHF, other products could be 4-hydroxypentanal, 2-hydroxy-5- methyltetrahydrofuran, 5-hydroxy-2-pentanone, 2,3-dihydro-2-methylfuran, 1-pentanol, and valeric acid, formed by subsequent hydrogenation/dehydration reaction (Scheme 2). This scheme will be discussed in Section 3.3.2.

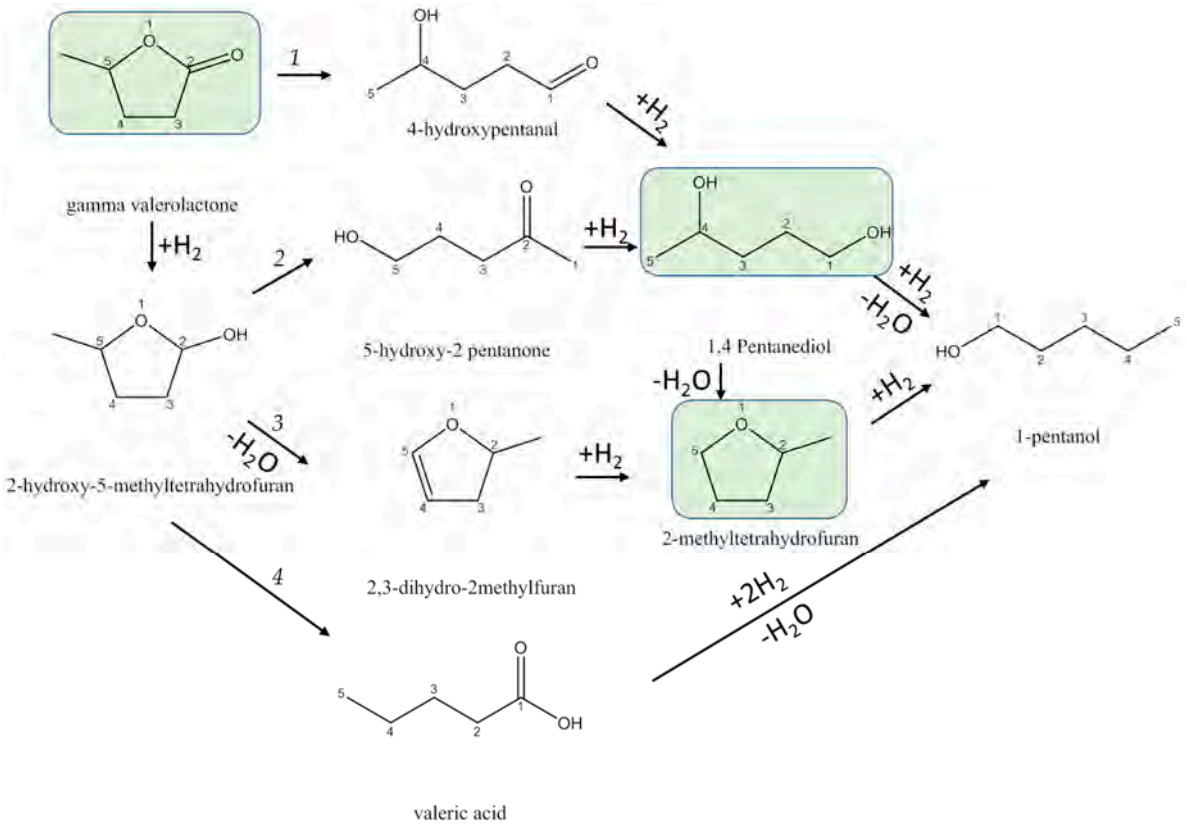

Scheme 2. Scheme of catalytic hydrogenation of GVL.

According to GLC analysis, the main reaction products in the current work were MTHF and PDO, while pentanol was observed with content not exceeding 0.5%; valeric acid and 2,3-dihydromethylfurane (DHMF) were observed only in experiments with noble metal catalysts in the level less 0.6%. GVL conversion was surprisingly very low at 393 K and 3.0 MPa, with the chosen substrate to metal ratio of 0.7–1.7 mol GVL/g_{Me}. Absence of PDO over Ru/H-beta was attributed to a high acidity of zeolite support, which promotes PDO to MTHF consecutive conversion similar to a fast intermolecular esterification-cyclization of 3-hydroxypentanoic acid benefitted by the zeolite acidity in LA hydrogenation to GVL [26]. Catalytic results are presented in Table S1 (Supplementary Materials), indicating a better selectivity to PDO in the presence of SiO_2 and Al_2O_3 supported catalysts, particularly bearing Ir, IrRe, PtRe, and Cu metals. A higher hydrogen pressure and lower temperatures applied for GVL hydrogenation promoted formation of PDO, while generation of MTHF predominately occurred at higher temperatures, being more pronounced in *n*-butanol (Table S1, entries 3 and 4). Interestingly, ZrO_2 as a support showed a better performance compared with alumina and ZnO among supported copper catalysts in the liquid-phase hydrogenation of GVL in ethanol at 200 °C in a batch reactor [43]. Some contradictions with the literature data not allowing a clear cut selection of the optimal catalyst on the basis of the obtained results demonstrate that catalytic activity can be affected by many reaction parameters such as solvent, temperature, pressure, the substrate to catalyst ratio, and hydrogen mass transfer.

3.3. Continuous Hydrogenation

Several advantages of the continuous operation compared with the batch mode are apparent, namely, in situ catalyst reduction and regeneration, low dependence on the use of a solvent, and absence of catalyst abrasion. Moreover there is no need for catalyst separation and utilization of high H_2 pressure.

Preliminary catalyst screening in a batch reactor showed feasibility of GVL hydrogenation into PDO over IrRe and Cu containing catalysts. Considering potential industrial implementation, a less expensive Cu/SiO_2 catalyst was selected for a further study in continuous GVL hydrogenation into PDO.

3.3.1. Effect of Process Parameters

To evaluate the influence of reaction conditions, the effect of temperature on GVL conversion and selectivity to PDO was studied first. Surprisingly, GVL conversion in 1,4-dioxane in a continuous mode was very low compared with that in *n*-butanol, thus the latter was used further. This difference can hardly be attributed to different hydrogen solubility or strong adsorption of one of the solvents blocking the active sites. Apparently, the effect of the solvent can tentatively be ascribed to a much more facile protonation in a polar protic solvent (i.e., *n*-butanol) in comparison with a low-polar aprotic 1,4-dioxane (Scheme 2). GVL hydrogenation was performed under the total H_2 pressure not exceeding 1.3 MPa, which is beneficial for the industrial application from the viewpoint of process safety and low production costs. It was observed that GVL concentration decreased with a temperature rise, while the PDO yield only slightly increased. At the same time, the yield of MTHF increased significantly (Figure 2). The amount of valeric acid was very low, being less than 0.05%, indicating a low contribution of 2-hydroxy-5-methylterahydrofurane transformation route through hydrogenolysis of the $-C_{CH3}-O-$ bond at the methyl side (Scheme 2). The reaction mixture contained only traces of pentanol (<0.5%) in this temperature range because dehydration generally occurs at temperatures higher than 473 K, as discussed in [21].

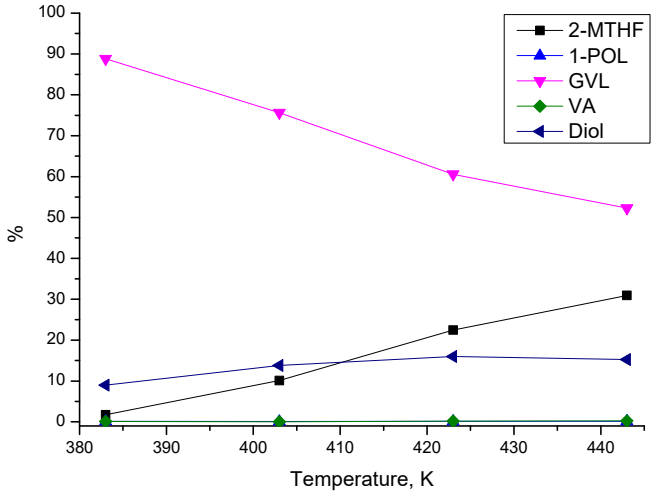

Figure 2. Effect of the reaction temperature on the reaction components' distribution in hydrogenation of γ-valerolactone (GVL) over Cu/SiO_2. Reaction conditions: 10.1% GVL in *n*-butanol, GVL feed rate of 2.1 g h^{-1}; catalyst weight of 0.455 g; H_2 pressure of 1.3 MPa; H_2 flow rate of 167 cm^3 min^{-1}. MTHF, 2-methyltetrahydrofuran; VA, valeric acid.

An increase in temperature led to an increase in GVL conversion, while selectivity to the desired PDO decreased and, simultaneously, selectivity to MHTF increased (Figure 3). Therefore, low temperatures such as below 413 K are preferred for the selective formation of PDO from GVL. The values of the apparent activation energy will be discussed below.

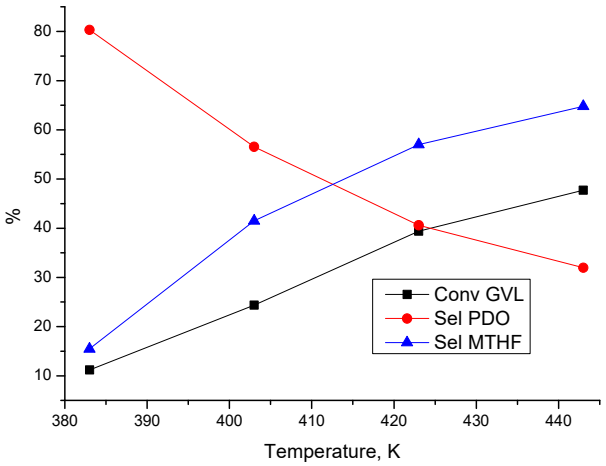

Figure 3. GVL conversion and selectivity to 1,4-pentanediol (PDO) and MTHF vs. reaction temperature over Cu/SiO_2. Reaction conditions: 10.1% GVL in *n*-butanol, GVL feed rate of 2.1 g h^{-1}; catalyst weight of 0.455 g; H_2 pressure of 1.3 MPa; H_2 flow rate of 167 cm^3 min^{-1}.

Similar dependences were observed by Sun et al. [21] in continuous GVL hydrogenation over a commercial Cu/ZnO catalyst (N211, Nikki Chemical Co., Ltd., Tokyo, Japan). Selectivity to PDO over Cu/ZnO decreased with increasing temperature, while selectivity to MTHF and 1-pentanol increased. Formation of the latter in these conditions could be attributed to the presence of basic sites in ZnO [21], which was not the case for SiO_2 used as a support for Cu in the current study. A lower selectivity to PDO over Cu/SiO_2 in the current work compared with that over Cu/ZnO [21] can be attributed to minor acidity of silanol groups in silica, favoring further conversion of PDO to MTHF to a larger extent compared with Cu/ZnO [21].

Catalytic runs at different H_2 flow rates (Figure 4) showed that GVL hydrogenation rate at the flow rate of 167 cm^3 min^{-1} resulted in a higher GVL conversion, yielding more PDO (Figure 4). An increase of the flow rate to 243 cm^3 min^{-1} did not affect GVL and slightly increased the PDO formation. A tentative explanation for such behavior is that initial elevation of the flow rate to 167 cm^3 min^{-1} increased the partial pressure of hydrogen, while a large excess of the latter can hinder adsorption of GVL at higher hydrogen flow rates. Earlier, Sun et al. [21] found an optimal H_2 flow rate of 90 cm^3 min^{-1} for GVL hydrogenation on Cu/ZnO. The difference could be attributed to different GVL feed rates and copper loadings as well as differences in the support contribution.

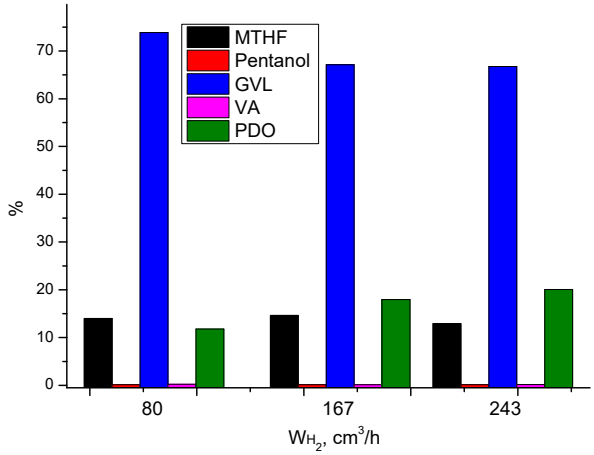

Figure 4. Composition of the reaction mixture depending on hydrogen flow rate in the hydrogenation of GVL over Cu/SiO_2. Reaction conditions: 10.1% GVL in *n*-butanol; GVL feed rate of 2.1 g h^{-1}; catalyst weight of 0.455 g; H_2 pressure of 1.3 MPa; temperature of 403 K; H_2 flow rate of 80, 167, and 240 cm^3 min^{-1}.

The effect of hydrogen pressure on the hydrogenation of GVL to PDO is presented in Figure 5. Similarly to various hydrogenation reactions, an increase of hydrogen pressure is beneficial for the hydrogenation rate, thus GVL conversion and selectivity to PDO and MTHF increased with increasing H_2 pressure. Moreover, selectivity to the latter products changed in a similar fashion with the H_2 pressure increase up to 1.3 MPa (Figure 6), demonstrating that their formation rates have similar reaction orders in hydrogen or both reactions rates have the same preceding rate-determining step, namely, hydrogenation of GVL into 2-hydroxy-5-methyltetrahydrofurane (Scheme 2).

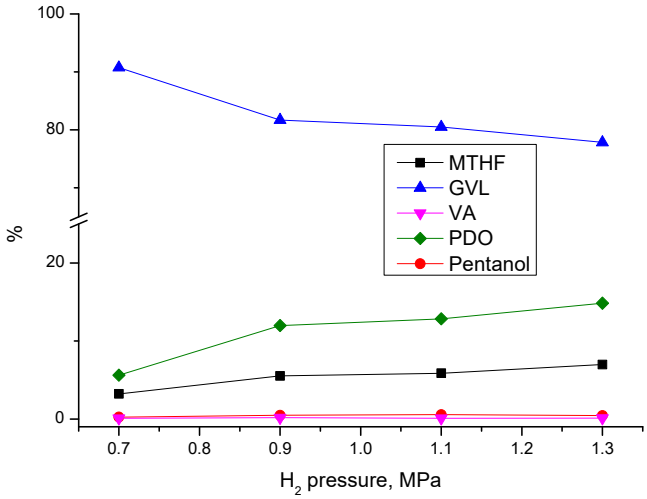

Figure 5. Composition of the reaction mixture vs. hydrogen pressure for hydrogenation of GVL over Cu/SiO_2. Reaction conditions: 10.1% GVL in *n*-butanol; GVL feed rate of 2.1 g h^{-1}; catalyst weight of 0.455 g; H_2 pressure of 1.3 MPa; temperature of 403 K; H_2 flow rate of 167 cm^3 min^{-1}.

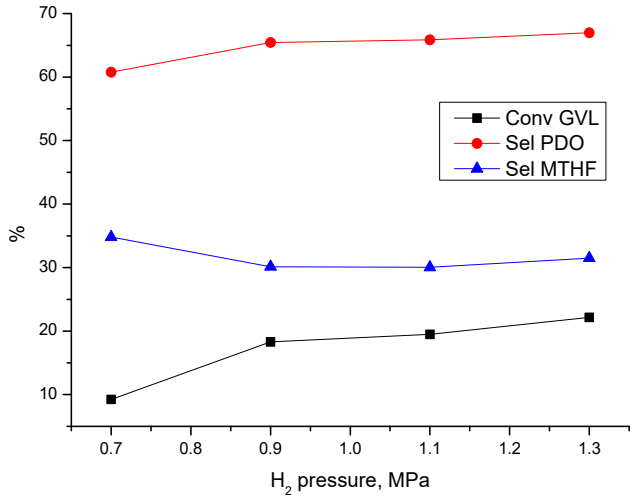

Figure 6. Conversion of GVL and selectivity to PDO and MTHF vs. hydrogen pressure in hydrogenation of GVL over Cu/SiO_2. Reaction conditions: 10.1% GVL in *n*-butanol; GVL feed rate of 2.1 g h^{-1}; catalyst weight of 0.455 g; H_2 pressure of 1.3 MPa; temperature of 403 K; H_2 flow rate of 167 cm^3 min^{-1}.

Maximum PDO selectivity of 67% obtained at GVL hydrogenation over Cu/SiO_2 was achieved at GVL conversion of 32% at 403 K and 1.3 MPa, while decreasing H_2 pressure to 0.7 MPa resulted in GVL conversion decrease to 9.4%, providing a slightly lower PDO selectivity of 61% (Figure 6).

3.3.2. Reaction Pathways

The effect of the contact time was studied at temperatures of 403, 413, 423, and 443 K. It was observed that the GVL content decreased at the expense of the content of the main products when

the contact time increased up to 1.6 h (Figure 7a–d). Figure S1 (Supplementary Material) displays the Arrhenius dependence. The apparent activation energy in GVL hydrogenation was estimated to be ca. 28.5 kJ/mol (87% confidence) (Figure S1), confirming the absence of at least external mass transfer limitations. Taking into account the absolute value of the activation energy and the size of catalyst particles (0.5–0.63 mm), the presence of internal mass transfer limitations cannot be ruled out. It follows from Figure 7a–d that the yields of PDO and MTHF changed with the contact time depending on the reaction temperature. The most plausible explanation of the observed behaviour is that, while PDO and MTHF are formed in parallel ways, at higher temperatures, there is a possibility of additional MTHF formation as a result of PDO dehydration. The rate of this reaction is apparently higher than the rate of PDO formation. This explanation agrees with the reaction mechanism proposed by Sun et al. [21], who considered that GVL hydrogenation can occur via four reaction routes (Scheme 2) including a parallel transformation into PDO and MTHF with a further conversion of PDO to MTHF.

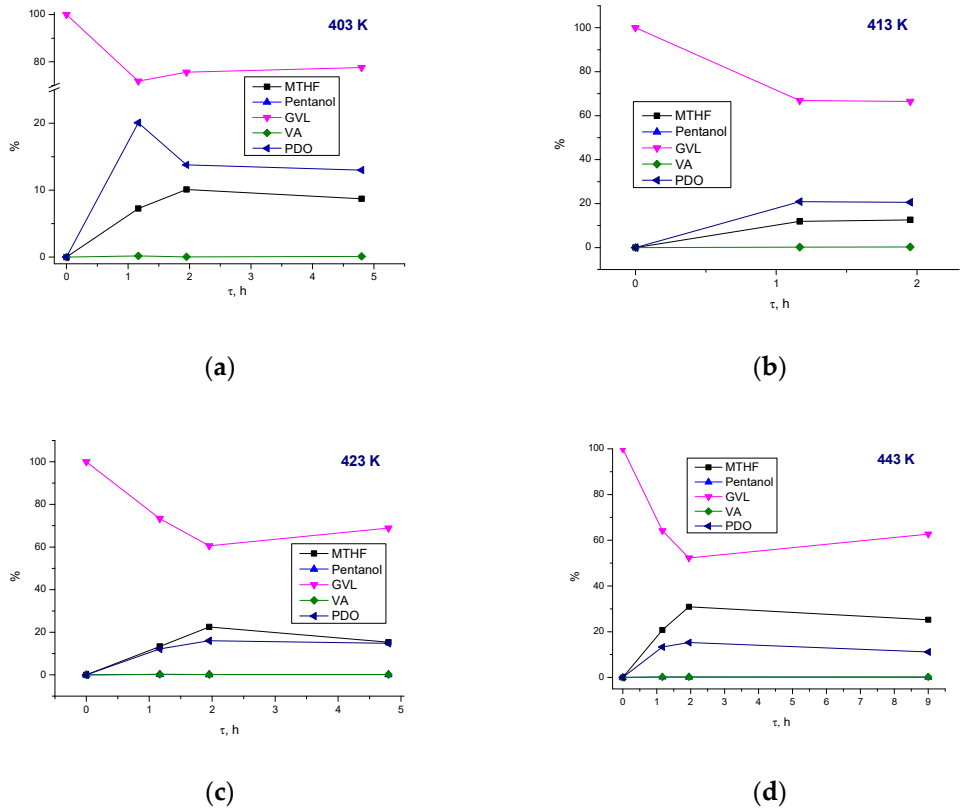

Figure 7. The composition of the reaction mixture vs. contact time in hydrogenation of GVL over Cu/SiO_2 at different temperatures (**a**) 403 K; (**b**) 413 K; (**c**) 423 K; and (**d**) 443 K. Reaction conditions: 10.1% GVL in *n*-butanol, catalyst weight of 0.455 g; H_2 pressure of 1.3 MPa; H_2 flow rate of 167 $cm^3 \cdot min^{-1}$.

Considering these routes in detail, the first route (*1*) includes a direct cleavage of -$C_{C=O}$-O- bond at the carbonyl side of GVL, resulting in 4-hydroxypentanal (HPL), whose consecutive hydrogenation results in PDO formation. The other three routes (*2*, *3*, *4*) comprise hydrogenation of the -C=O carbonyl bond of GVL into -C-OH group, resulting in the intermediate 2-hydroxy-5-methyltetrahydrofuran (HMTHF). Subsequently, the second route (*2*) includes a consecutive ring opening of HMTHF to 5-hydroxy-2-pentanone (HPN) by hydrogenolysis of the -$C_{C\text{-}OH}$-O- bond at the hydroxyl side of HMTHF, followed by hydrogenation to PDO. The third route (*3*) involves dehydration of HMTHF, resulting in 2,3-dihydro-2-methylfuran (DHMF), where the ring -C=C- double bond is further saturated, giving 2-methyltetrahydrofuran (MTHF) followed by the ring hydrogenolysis into 1-pentanol. The fourth route (*4*) involves the ring opening of HMTHF through the cleavage of -C_{CH3}-O- bond at the methyl side, forming valeric acid (VA), which can be further converted into pentanols. Both VA and

HPN are the ring-opening products of HMTHF; the cleavage of -C_{CH3}-O- bond at the methyl side results in VA, and hydrogenolysis of -$C_{C\text{-}OH}$-O- bond at the hydroxyl side leads to HPN. Note that HPL and HPN could both be PDO intermediates with a higher probability for HPL, considering that the carbonyl group of aldehydes is more prone to hydrogenation than the keto group [44]. PDO can be further transformed to MTHF and pentanol by dehydration and hydrogenation, correspondingly. Thus, PDO and DHMF could both be MTHF intermediates. Analysis of the product distribution depending on the metal applied allowed to suggest that the reaction on Cu/ZnO mainly follows routes (*1*, *2*), while routes (*3*, *4*) are preferred over Ni and Pd catalysts [21].

In the current study, neither VA nor HPN were detected in the reaction mixture during GVL hydrogenation over Cu/SiO_2, while pentanol was detected at a low level of 0.5%. These results are in accordance with the product distribution obtained by Sun et al. in hydrogenation of neat GVL over commercial Cu/SiO_2 (G-108B, Clariant Catalysts, Japan) [21]. However, even at low temperatures and low GVL conversion, formation of MTHF was observed along with PDO. This is probably a feature of the Cu/SiO_2 catalyst applied in this study as the crystal structure of Cu-Si precursor corresponded to the mineral chrysocolla with a negligible amount of over-stoichiometric silica. Subsequently, the reductive activation leads to the formation of highly dispersed and active Cu^0 nanoparticles with reversible RedOx properties along with a highly developed surface area of 520 m^2/g [29]. This could favor transformations of GVL into PDO, followed by formation of a thermodynamically controlled mixture of PDO and MTHF. The composition of such a mixture is influenced by formation of water also in routes *2* and *3*, giving overall a predominant excess of PDO at low temperatures and a higher content MTHF at higher temperatures. Note that the Cu/SiO_2 catalyst applied in this study exhibited unusual bifunctional properties in hydrogenation of methyl lactate, resulting in the 1,2-propanediol yield of 76% [29].

3.3.3. Stability of Cu/SiO_2 Catalyst

Separate experiments were carried out in the fixed-bed reactor to study the stability of Cu/SiO_2 with time-on-stream (TOS) at the same contact time. According to the experimental data, the content of GVL decreases rather slowly, while the yield of PDO increased slightly (Figure 8). The reduction of copper cations in the silicate precursor is irreversible, resulting in the oxygen anions' removal as water molecules. This explanation is in line with a rather slow catalyst deactivation and apparently high steady state activity. Cu particles oxidized during the reaction can be reduced reversibly after a treatment by molecular hydrogen at 523 K (2 h), thereby restoring catalytic activity, as shown experimentally. Selectivity to PDO was almost the same with TOS indicating no changes of the microstructure of the active copper sites responsible for PDO formation, whereas the total amount of active sites probably decreased as a result of deposition of formed side products. A rather stable catalytic activity can be explained by a partial decoration of the highly dispersed metal particles with silicon oxohydroxide particles of the support, thereby preventing migration of copper particles during hydrogenation. Moreover, according to XRF, Cu^0 leaching of ca. 2.5% was observed during 9 h TOS. That could be explained by suppression of GVL transformations to valeric acid (route *3*) according to the reaction scheme (Scheme 2), as the acids are known to efficiently form complexes with copper facilitating its leaching. Note that the leached Cu might be more active as well, and thus obscure deactivation of the heterogeneous catalyst.

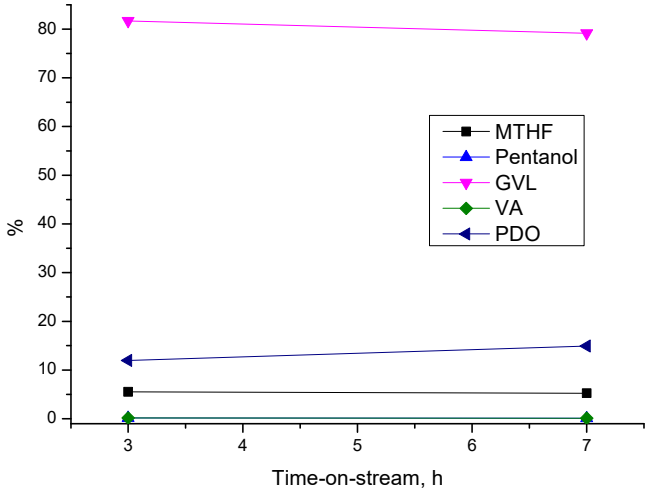

Figure 8. Composition of the reaction mixture vs. time-on-stream in hydrogenation of GVL over Cu/SiO_2. Reaction conditions: 10.1% GVL in *n*-butanol; GVL feed rate of 2.1 g h^{-1}; catalyst weight of 0.455 g; H_2 pressure of 0.9 MPa; temperature of 403 K; H_2 flow rate of 167 cm^3 min^{-1}.

3.4. XRD of Cu/SiO_2 before and after the Reaction

XRD analysis of Cu/SiO_2 before and after the reaction is presented in Table 1 and Figure 9. The as-prepared and freshly reduced at 653 K Cu/SiO_2 catalyst showed the presence of a highly dispersed crystallographic phase of Cu^0 (space group Fm-3m) with the elementary cubic cell parameter a = b = c = 3.613(2) Å, lattice angles $\alpha = \beta = \gamma = 90°$ close to metallic copper lattice parameters. Diffraction peaks referring to Cu_2O (space group Pn-3m) were observed with a significantly decreased value of the unit cell parameter a = b = c = 4.269 Å indicating cationic modification, while no changes in the lattice angles were observed $\alpha = \beta = \gamma = 90°$. This seems to be typical for the Cu-Si catalyst obtained by reduction of the oxide precursor of copper hydroxysilicate with a chrysocolla structure. Coherently scattering domains (CSD) of Cu^0 and Cu_2O phases were 6.5 and 2.5 nm, correspondingly (Table 1). An intense diffraction peak with a maximum at $2\theta = 26.6°$ in the freshly reduced catalyst was related to the quartz phase SiO_2 (PDF # 00-046-1045) with the coherently scattering domain (CSD) exceeding 100 nm. The spent catalyst Cu/SiO_2 exhibited presence of Cu^0 with the elementary cell parameter a = b = c = 3.615(1) Å, and the lattice angles $\alpha = \beta = \gamma = 90°$ typical for the metallic copper lattice parameters. The structure of Cu_2O phase was rearranged under the influence of the reaction media and the value of the lattice parameter approaches the value characteristic for Cu_2O (a = b = c = 4.266(2)Å, $\alpha = \beta = \gamma = 90°$). The X-ray amorphous SiO_2 phase has disappeared after the reaction. The CSD values of Cu^0 and Cu_2O in the spent catalyst were found to be 31.0 and 4.0 nm (Table 1), respectively, indicating that the copper particles in these samples were covered with a thin film of copper oxide, while during the reaction, coalescence of metallic copper particles was observed. The molar ratio of the metallic and oxidized copper phases decreased after the reaction, indicating that oxidation of copper particles occurred along with their sintering. Reductive regeneration of the spent catalyst by thermal treatment by molecular hydrogen enabled restoration of catalytic activity, mainly because the oxidized surface copper layers could be fairly well reduced under appropriate reductive conditions.

Table 1. X-ray diffraction (XRD) analysis of freshly reduced and spent Cu/SiO_2 catalysts.

Catalyst	CSD, nm		Phase Content, wt.%		Molar Ratio of Phases	Unit Cell Parameter a = b = c, Å, Determined/Standard	
	Cu^0	Cu_2O	Cu^0	Cu_2O	Cu^0/Cu_2O	Cu^0	Cu_2O
Cu/SiO_2 fresh	6.5	2.5	30	70	~1/1	3.613(2)/3.615	4.225(3)/4.269
Cu/SiO_2 spent	31.0	4.0	7	93	~1/6	3.615(1)/3.615	4.266(2)/4.269

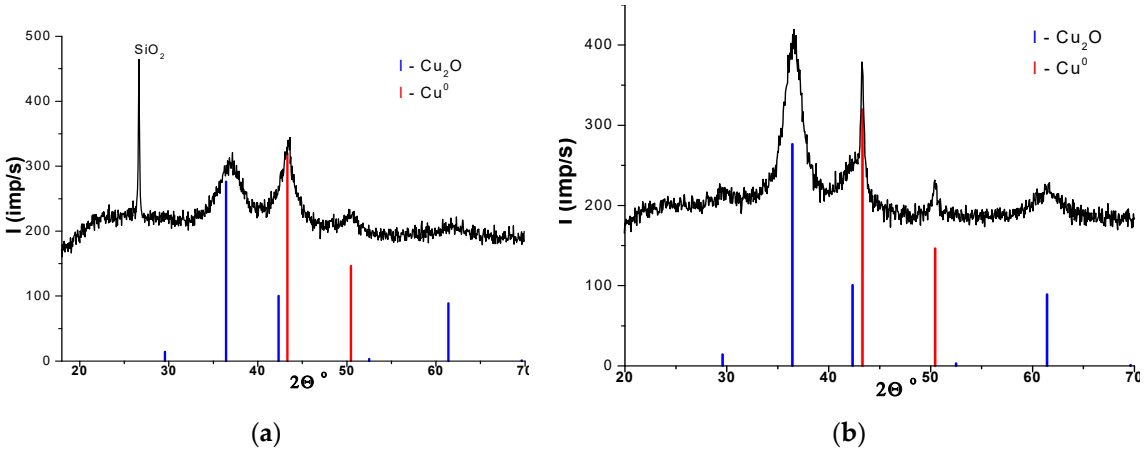

Figure 9. Diffraction patterns of the catalysts in comparison with the position and relative intensity of the crystallographic phases Cu^0 and Cu_2O: (**a**) Cu/SiO_2 freshly reduced; (**b**) Cu/SiO_2 spent.

4. Conclusions

Hydrogenation of γ-valerolactone (GVL) in polar solvents (*n*-butanol, 1,4-dioxane) to 1,4-pentanediol (PDO) and 2-methyltetrahydrofuran (MTHF) was performed at 363–443K in a fixed bed reactor under overall H_2 pressure of 0.7–1.3 MPa. Preliminary screening in a batch reactor was performed in comparable reaction conditions with a series of Ru, Ir, Pt, Co, and Cu catalysts, earlier efficiently applied for levulinic acid hydrogenation to GVL. Among the catalysts, Cu/SiO_2 provided better selectivity of 67% towards PDO at 32% GVL conversion in a continuous flow reactor using *n*-butanol as a solvent. This catalyst was applied to study the effect of temperature, hydrogen pressure, and contact time. The main reaction products were PDO, MTHF, and 1-pentanol, while no valeric acid was observed. While Cu/SiO_2 activity slightly decreased with time-on-stream (9 h) as a result of a partial oxidation of metallic copper, it can be restored after treatment by molecular hydrogen at 523 K (2 h), demonstrating fair catalyst stability.

Summarizing all experimental observations and literature data, it is inferred that PDO formation can be selectively achieved over silica supported copper bifunctional catalysts in mild conditions. The acidity of silica supported catalyst could be balanced by the Cu/Si ratio, Cu loading, and preparation conditions, e.g., temperature of the reductive activation. This finding opens a promising way to develop an efficient approach for biogenic diols' preparation as an alternative to currently applied petroleum-based method, as well as to integrate GVL into PDO stage into biorefinery strategy realizing in mild reaction conditions.

Supplementary Materials: The following are available online at http://www.mdpi.com/2624-781X/1/2/6/s1, Table S1: Liquid-phase GVL hydrogenation in a batch mode. Reaction conditions: GVL (6.9 mmol), solvent (15 mL), m_{cat} = 0.24 g, T = 393 K, PH_2 = 3.0 MPa, time = 4 h; Figure S1: Temperature dependence in the Arrhenius coordinates. Reaction conditions: 10.1% GVL in *n*-butanol, GVL feed rate 2.1 g h^{-1}; catalyst weight, 0.455 g; H_2 pressure 1.3 MPa; H_2 flow rate 167 cm^3 min^{-1}.

Author Contributions: Conceptualization, I.S. and V.B.; Methodology, D.Y.M.; Formal Analysis, S.P.; Investigation, Y.D. and M.S.; Resources, P.D.; Data Curation, P.N. and Y.D.; Writing—Original Draft Preparation, Y.D. and I.S.; Writing—Review & Editing, D.Y.M.; Visualization, S.P. and M.S.; Supervision, I.S., P.D., and V.B.; Project Administration, I.S. and V.B.; Funding Acquisition, V.B. and I.S. All authors have read and agreed to the published version of the manuscript.

Funding: This work was supported by RFBR Grant 18-53-45013 IND_a. Funding under INT/RUS/RFBR/P-323 project is acknowledged.

Acknowledgments: The authors thank engineer O.G. Arkhipova (experimental assistance), E. Gerasimov (TEM), N. Shtertser (H_2-TPR), I. Krayevskaya (XRF), and A. Leonova (N_2 physisorption) for catalysts' characterization, and V.A. Utkin, for GC/MS analysis. The authors wish to express their gratitude to T.P. Minyukova for providing characterization data of Cu/SiO_2 and helpful discussions.

Conflicts of Interest: The authors declare no conflict of interest. The funders had no role in the design of the study; in the collection, analyses, or interpretation of data; in the writing of the manuscript; or in the decision to publish the results.

References

1. Mäki-Arvela, P.; Holmbom, B.; Salmi, T.; Murzin, D.Y. Recent progress in synthesis of fine and specialty chemicals from wood and other biomass by heterogeneous catalytic processes. *Catal. Rev. Sci. Eng.* **2007**, *49*, 197–340. [CrossRef]
2. Bozell, J.J.; Moens, L.; Elliott, D.C.; Wang, Y.; Neuenscwander, G.G.; Fitz-Patrick, S.W.; Bilski, R.J.; Jarnefeld, J.L. Production of levulinic acid and use as a platform chemical for derived products. *Resour. Conserv. Recycl.* **2000**, *28*, 227–239. [CrossRef]
3. De Souza, R.O.M.A.; Miranda, L.S.M.; Luque, R. Bio (chemo) technological strategies for biomass conversion into bioethanol and key carboxylic acids. *Green Chem.* **2014**, *16*, 2386–2405. [CrossRef]
4. Werpy, T.; Petersen, G. *Top Value Added Chemicals from Biomass: Volume I—Results of Screening for Potential Candidates from Sugars and Synthesis Gas (No. DOE/GO-102004-1992)*; US Department of Energy: Golden, CO, USA, 2004. Available online: https://www.nrel.gov/docs/fy04osti/35523.pdf (accessed on 15 October 2020).
5. Simakova, I.L.; Murzin, D.Y. Transformation of bio-derived acids into fuel-like alkanes via ketonic decarboxylation and hydrodeoxygenation: Design of multifunctional catalyst, kinetic and mechanistic aspects. *J. Energy Chem.* **2016**, *25*, 208–224. [CrossRef]
6. Han, J. Process design and techno-economic evaluation for catalytic production of cellulosic γ-valerolactone using lignin derived propyl guaiacol. *J. Ind. Eng. Chem.* **2017**, *52*, 218–223. [CrossRef]
7. Hong, M.; Chen, E.Y.-X. Chemically recyclable polymers: A circular economy approach to sustainability. *Green Chem.* **2017**, *19*, 3692–3706. [CrossRef]
8. Westhues, S.; Idel, J.; Klankermayer, J. Molecular catalyst systems as key enablers for tailored polyesters and polycarbonate recycling concepts. *Sci. Adv.* **2018**, *4*, eaat9669. [CrossRef]
9. Du, X.-L.; Bi, Q.-Y.; Liu, Y.-M.; Cao, Y.; He, H.-Y.; Fan, K.-N. Tunable copper-catalyzed chemoselective hydrogenolysis of biomass-derived γ-valerolactone into 1,4-pentanediol or 2-methyltetrahydrofuran. *Green Chem.* **2012**, *14*, 935–939. [CrossRef]
10. Ahn, Y.-C.; Han, J. Catalytic production of 1,4-pentanediol from corn stover. *Bioresour. Technol.* **2017**, *245*, 442–448. [CrossRef]
11. Geilen, F.M.A.; Engendahl, B.; Harwardt, A.; Marquardt, W.; Klankermayer, J.; Leitner, W. Selective and flexible transformation of biomass-derived platform chemicals by a multifunctional catalytic system. *Angew. Chem.* **2010**, *122*, 5642–5646. [CrossRef]
12. Delidovich, I.; Leonhard, K.; Palkovits, R. Cellulose and hemicellulose valorisation: An integrated challenge of catalysis and reaction engineering. *Energy Environ. Sci.* **2014**, *7*, 2803–2830. [CrossRef]
13. Vom Stein, T.; Meuresch, M.; Limper, D.; Schmitz, M.; Hoelscher, M.; Coetzee, J.; Cole-Hamilton, D.J.; Klankermayer, J.; Leitner, W. Highly versatile catalytic hydrogenation of carboxylic and carbonic acid derivatives using a Ru-triphos complex: Molecular control over selectivity and substrate scope. *J. Am. Chem. Soc.* **2011**, *36*, 13217–13225.
14. Li, W.; Xie, J.-H.; Yuan, M.-L.; Zhou, Q.-L. Ruthenium complexes of tetradentate bipyridine ligands: Highly efficient catalysts for the hydrogenation of carboxylic esters and lactones. *Green Chem.* **2014**, *16*, 4081–4085. [CrossRef]
15. Krstanje, T.J.; van der Vlugt, J.I.; Elsevier, C.J.; de Bruin, B. Hydrogenation of carboxylic acids with a homogeneous cobalt catalyst. *Science* **2015**, *350*, 298–302. [CrossRef]
16. Srimani, D.; Mukherjee, A.; Goldberg, A.F.G.; Leitus, G.; Diskin-Posner, Y.; Shimon, L.J.W.; David, Y.B.; Milstein, D. Cobalt-catalyzed hydrogenation of esters to alcohols: Unexpected reactivity trend indicates ester enolate intermediacy. *Angew. Chem. Int. Ed.* **2015**, *54*, 12357–12360. [CrossRef]
17. Elangovan, S.; Wendt, B.; Topf, C.; Bachmann, S.; Scalone, M.; Spannenberg, A.; Jiao, H.; Baumann, W.; Junge, K.; Beller, M. Improved second generation iron pincer complexes for effective ester hydrogenation. *Adv. Synth. Catal.* **2016**, *358*, 820–825. [CrossRef]

18. Al-Shaal, M.G.; Dzierbinski, A.; Palkovits, R. Solvent-free γ-valerolactone hydrogenation to 2-methyltetrahydrofuran catalysed by Ru/C: A reaction network analysis. *Green Chem.* **2014**, *16*, 1358–1364. [CrossRef]
19. Mizugaki, T.; Nagatsu, Y.; Togo, K.; Maeno, Z.; Mitsudome, T.; Jitsukawa, K.; Kaneda, K. Selective hydrogenation of levulinic acid to 1,4-pentanediol in water using a hydroxyapatite-supported Pt–Mo bimetallic catalyst. *Green Chem.* **2015**, *17*, 5136–5139. [CrossRef]
20. Li, M.; Li, G.; Li, N.; Wang, A.; Dong, W.; Wang, X.; Cong, Y. Aqueous phase hydrogenation of levulinic acid to 1,4-pentanediol. *Chem. Commun.* **2014**, *50*, 1414–1416. [CrossRef]
21. Sun, D.; Saito, T.; Yamada, Y.; Chen, X.; Sato, S. Hydrogenation of γ-valerolactone to 1,4-pentanediol in a continuous flow reactor. *Appl. Catal. A Gen.* **2017**, *542*, 289–295. [CrossRef]
22. Xue-jiao, Z.; Chuang, L.; Xin, D.; Dong-dong, Y.; Chang-hai, L. Preparation of Cu/MgO catalysts for γ-valerolactone hydrogenation to 1,4-pentanediol by MOCVD. *J. Fuel Chem. Technol.* **2017**, *45*, 537–546.
23. Xu, Q.; Li, X.; Pan, T.; Yu, C.; Deng, J.; Guo, Q.; Fu, Y. Supported copper catalysts for highly efficient hydrogenation of biomass-derived levulinic acid and γ-valerolactone. *Green Chem.* **2016**, *18*, 1287 1294. [CrossRef]
24. Wu, J.; Gao, G.; Li, Y.; Sun, P.; Wang, J.; Li, F. Highly chemoselective hydrogenation of lactone to diol over efficient copper-based bifunctional nanocatalysts. *Appl. Catal. B Environ.* **2019**, *245*, 251–261. [CrossRef]
25. Simakova, I.L.; Demidova, Y.S.; Simonov, M.N.; Niphadkar, P.S.; Bokade, V.V.; Devi, N.; Dhepe, P.L.; Murzin, D.Y. Carbon supported size-controlled ru catalysts for selective levulinic acid hydrogenation into γ-valerolactone. *J. Sib. Fed. Univ. Chem.* **2020**, *13*, 5–16. [CrossRef]
26. Simakova, I.L.; Demidova, Y.S.; Simonov, M.N.; Niphadkar, P.S.; Bokade, V.V.; Devi, N.; Dhepe, P.L.; Murzin, D.Y. Mesoporous carbon and microporous zeolite supported Ru catalysts for selective levulinic acid hydrogenation into γ-valerolactone. *Catal. Sustain. Energy* **2019**, *6*, 38–49. [CrossRef]
27. Yurieva, T.M.; Kustova, G.N.; Minyukova, T.P.; Poels, E.K.; Bliek, A.; Demeshkina, M.P.; Plyasova, L.M.; Kriger, T.A.; Zaikovskii, V.I. Non-hydrothermal synthesis of copper-, zinc and copper-zinc hydrosilicates. *Mater. Res. Innov.* **2001**, *5*, 3–11. [CrossRef]
28. Minyukova, T.P.; Khassin, A.A.; Yurieva, T.M. Controlling the catalytic properties of copper-containing oxide catalysts. *Kinet. Catal.* **2018**, *59*, 112–122. [CrossRef]
29. Simonov, M.N.; Zaikin, P.A.; Simakova, I.L. Highly selective catalytic propylene glycol synthesis from alkyl lactate over copper on silica: Performance and mechanism. *Appl. Catal. B Environ.* **2012**, *119*, 340–347. [CrossRef]
30. Bart, J.C.J.; Sneeden, R.P.A. Copper-zinc oxide-alumina methanol catalysts revisited. *Catal. Today* **1987**, *2*, 1–124. [CrossRef]
31. Turek, T.; Trimm, D.L.; Cant, N.W. The catalytic hydrogenolysis of esters to alcohols. *Catal. Rev. Sci. Eng.* **1994**, *36*, 645–683. [CrossRef]
32. Rhodes, C.; Hutchings, G.J.; Ward, A.M. Water-gas shift reaction: Finding the mechanistic boundary. *Catal. Today* **1995**, *23*, 43–58. [CrossRef]
33. Shao, Y.; Sun, K.; Li, Q.; Liu, Q.; Zhang, S.; Liu, Q.; Hu, G.; Hu, X. Copper-based catalysts with tunable acidic and basic sites for the selective conversion of levulinic acid/ester to γ-valerolactone or 1,4-pentanediol. *Green Chem.* **2019**, *21*, 4499–4511. [CrossRef]
34. Nieminen, V.; Karhu, H.; Kumar, N.; Heinma, I.; Ek, P.; Samoson, A.; Salmi, T.; Murzin, D.Y. Physico-chemical and catalytic properties of Zr- and Cu-Zr ion-exchanged H-MCM-41. *Phys. Chem. Chem. Phys.* **2004**, *6*, 4062–4069. [CrossRef]
35. Evans, J.W.; Wainwright, M.S.; Bridgewater, A.J.; Young, D.J. On the determination of copper surface area by reaction with nitrous oxide. *Appl. Catal. A Gen.* **1983**, *7*, 75–83. [CrossRef]
36. Simakova, O.A.; Simonov, P.A.; Romanenko, A.V.; Simakova, I.L. Preparation of Pd/C catalysts via deposition of palladium hydroxide onto Sibunit carbon and their application to partial hydrogenation of rapeseed oil. *React. Kinet. Catal. Lett.* **2008**, *95*, 3–12. [CrossRef]
37. Zaytseva, Y.A.; Panchenko, V.N.; Simonov, M.N.; Shutilov, A.A.; Zenkovets, G.A.; Renz, M.; Simakova, I.L.; Parmon, V.N. Effect of gas atmosphere on catalytic behaviour of zirconia, ceria and ceria-zirconia catalysts in valeric acid ketonization. *Top. Catal.* **2013**, *56*, 846–855. [CrossRef]

38. Mäki-Arvela, P.; Martin, G.; Simakova, I.; Tokarev, A.; Wärnå, J.; Hemming, J.; Holmbom, B.; Salmi, T.; Murzin, D.Y. Kinetics, catalyst deactivation and modeling in the hydrogenation of β-sitosterol to β-sitostanol over microporous and mesoporous carbon supported Pd catalysts. *Chem. Eng. J.* **2009**, *154*, 45–51.
39. Panchenko, V.N.; Paukshtis, E.A.; Murzin, D.Y.; Simakova, I.L. Solid base assisted n-pentanol coupling over VIII group metals: Elucidation of the Guerbet reaction mechanism by DRIFTS. *Ind. Eng. Chem. Res.* **2017**, *56*, 13310–13321. [CrossRef]
40. Simonov, M.N.; Simakova, I.L.; Minyukova, T.P.; Khassin, A.A. Hydrogenation of lactic acid on reduced copper-containing catalysts. *Russ. Chem. Bull.* **2009**, *58*, 1114–1118. [CrossRef]
41. Yurieva, T.M.; Minyukova, T.P.; Kustova, G.N.; Plyasova, L.M.; Kriger, T.A.; Demeshkina, M.P.; Zaikovskii, V.I.; Malakhov, V.V.; Dovlitova, L.S. Copper ions distribution in synthetic copper-zinc hydrosilicate. *Mater. Res. Innov.* **2001**, *5*, 74–80. [CrossRef]
42. Huang, X.; Cant, N.W.; Wainwright, M.S.; Ma, L. The dehydrogenation of methanol to methyl Formate—Part I: Kinetic studies using copper-based catalysts. *Chem. Eng. Process.* **2005**, *44*, 393–402.
43. Sun, D.; Takahashi, Y.; Yamada, Y.; Sato, S. Efficient formation of angelica lactones in a vapor-phase conversion of levulinic acid. *Appl. Catal. A Gen.* **2016**, *526*, 62–69. [CrossRef]
44. Akiyama, M.; Sato, S.; Takahashi, R.; Inui, K.; Yokota, M. Dehydration–hydrogenation of glycerol into 1,2-propanediol at ambient hydrogen pressure. *Appl. Catal. A Gen.* **2009**, *371*, 60–66. [CrossRef]